Energy 76 (2014) 679–693

Contents lists available at ScienceDirect

Energy

journal homepage: www.elsevier.com/locate/energy

Novel fuzzy logic based sensorless maximum power point tracking strategy for wind turbine systems driven DFIG (doubly-fed induction generator)

K. Belmokhtar, M.L. Doumbia*, K. Agbossou

Hydrogen Research Institute, Université du Québec à Trois-Rivières, (P.O. Box 500), Trois-Rivières, Québec G9A 5H7, Canada

ARTICLE INFO

Article history:
Received 29 April 2014
Received in revised form
16 August 2014
Accepted 18 August 2014
Available online 15 September 2014

Keywords:
MPPT algorithm
WECS
Sensorless control
Fuzzy logic
MRAS
DFIG serial communication

ABSTRACT

This paper presents a novel FLC MPPT (fuzzy logic sensorless maximum power point tracking) method for WECS (wind energy conversion systems). The proposed method greatly reduces the speed variation range of the wind generator which leads to the downsizing the PWM (pulse width modulation) back-to-back converters by approximately 40% in comparison with conventional techniques. The method also increases the system's reliability by reducing the converter losses. Firstly, a MRAS (model reference adaptive system) based on fuzzy logic technique is used to estimate the DFIG (doubly-fed induction generator) rotor's speed. Then, a FLC MPPT (Fuzzy Logic Maximum Power Point Tracking) method is applied to provide the reference electromagnetic torque. Subsequently, in order to achieve the overall sensorless MPPT technique, the wind power is approximated from estimated generator speed and the reference of electromagnetic torque. Finally, the wind speed is estimated from the mechanical power using a fuzzy logic technique. The proposed control method has been applied to a WTG (wind turbine generator) driving a 3.7 kW DFIG in variable speed mode. In order to validate the simulation results, experimental tests have been performed on a 3.7 kW test bench, consisting of a DFIG and DC motor drive.

1. Introduction

Rising cost of fossil fuels and the need to reduce CO_2 emissions, especially in industrialized countries [1], have led to search for alternative energy sources such as wind energy which is considered as one of the most cost-effective renewable sources [2–6]. Wind turbines generated about 1.5% of global electricity consumption, with an installed capacity of 121 GW by the end of 2008 in more than 70 countries [7].

There are many major issues facing the design of WECS (wind energy conversion system). The first one is the significant wind speed variations at different points over the blades swept area which makes difficult any direct measurement of effective wind speed [8,9]. Furthermore, using mechanical sensors increases the cost of both equipment and maintenance, and reduces the reliability of the wind system [9–11]. To overcome these issues, some studies [8] have proposed to estimate the effective wind speed indirectly by using other signals, such as output power, electric torque, generator rotor's speed which are easy to measure [11], and combined with a dynamic model of wind turbine [12–14]. This approach has some drawback, since the wind turbine model is nonlinear and its parameters are difficult to find. Moreover, the wind speed can be estimated through system identification, state observer, data mining, and fuzzy techniques [8,10]. In Ref. [14], the wind speed estimation method based on the linearized model using a filter and a Newton's search algorithm. Nevertheless, the simulation result has not proved the stability or the convergence of the estimator.

In Ref. [10], Gaussian radial basis functions network dependent on the knowledge of the mechanical power, the turbine speed and the blade pitch angle have been proposed. However, this method which relies on the output power measurement and the power losses estimation, does not take into account the case where the output power is limited if the wind speed is above its rated power by pitch control system. A Neuro-fuzzy method to find wind speed profiles up to the height of 100 m based on the knowledge of wind speed at heights 10, 20, 30, 40 m is reported in Ref. [15], but the use of sensors increases the cost of the system.

This work presents a new strategy to compute the wind speed based on the estimation of the DFIG (doubly fed-induction

* Corresponding author. Tel.: +1 819 376 5011x3912; fax: +1 819 376 5219.
E-mail addresses: Kbelmokhtar@eolien.qc.ca (K. Belmokhtar), Mamadou.Doumbia@uqtr.ca (M.L. Doumbia), Kodjo.Agbossou@uqtr.ca (K. Agbossou).

http://dx.doi.org/10.1016/j.energy.2014.08.066
0360-5442/

generator) rotor's speed and its electromagnetic torque given by the fuzzy logic technique. The method allows the computation of wind speed even if it is above its rated value as reported by Ref. [10], which is due to limitation of output power at the rated value with pitch control system.

The rotor speed signal can be obtained by a number of methods such as speed sensor or using simple open loop speed estimator. Both of these methods have some drawbacks. The first method has a mechanical coupling problem and it is costly due to the use of a sensor and a connection cable. For the second method, the accuracy of speed estimation depends strongly on the machine parameters [16]. Sensorless speed and position estimation of the DFIG, based on the rotor or air gap flux linkage with integration calculation, have some drawbacks. Indeed, if the generator operates around synchronous speed, its rotor is excited with low frequency voltages, and the integrator cannot give an accurate output value. Then, it causes the failure of flux-linkage based control strategies [17,18]. In this paper, we propose a MRAS (model reference adaptive system) speed estimation observer based on the fuzzy logic controller which can take into account the errors from machine parameters variation [19]. To achieve the sensorless maximization of output power, a MRAS (model reference adaptive system) observer is used to estimate the rotor speed of the DFIG [20–23]. As reported in Ref. [24], many techniques have been developed for sensorless control of induction machines and for PMSG (permanent magnet synchronous generator)applications [24]. In Refs. [25], a MRAS using PI (proportional-integral) controller to estimate the DFIG rotor speed with low transient speed tracking is presented. In Ref. [26], a speed estimator based on adaptive fuzzy logic control technique is proposed. The drawback of this method is that the initial error of the starting period leads to a large percentage of error on the rotor speed value [27]. In Ref. [14] a nonlinear static state feedback with PI controller is proposed for a wind turbine driving a DFIG. However, this approach shows large errors between actual and estimated values. In order to improve the performance of the closed loop MRAS observe, a fuzzy logic controller is proposed in this paper.

In the aim to capture the maximum electrical power, the speed of the WTG (Wind Turbine Generator) must be adjusted to reach the optimal value of the tip speed ratio [28]. In literature survey, a large number of MPPT (Maximum Power Point Tracking) algorithms are presented in order to extract a maximum output power, and it can be classified into four most control approaches [29,30]. The first one, is the TSR (tip speed ratio) control, which regulates the rotor speed, with keeping TSR at its optimum value with the aim to capture the maximum wind power [10,31–36]. This method requires an accurate knowledge of the wind turbine parameters and the measurement of the wind speed to provide the value of the generator's speed to extract a maximum power. In Refs. [31,32] the tip-speed ratio is fixed at its optimal value λ_{opt} to achieve the maximum output power extraction giving thus the maximum power coefficient. This method is faced to some drawbacks, such as the impossibility to adapt the speed of the wind generator in the case of fast variation of the wind speed, due to its inertia. In Ref. [10] another method is presented where λ_{opt} is calculated from the roots of the derivative of the power coefficient relation C_p. This method is mainly limited by time consumption and calculation complexity, especially when the mathematical representation of the C_p is a fourth-order polynomial. Many C_p relations are reported in the literature such as the Eq. (8) (used in the present study) where the roots of its derivatives are difficult to obtain. The second method is the Perturb and Observe (P&O) method which is mainly used in a PV array MPPT algorithm [37], is a simple strategy to implement and low cost [38], does not require prior knowledge of neither wind speed nor generator's parameters [4,39–44]. Nevertheless, this MPPT algorithm has not a good tracking performance, and then, some new methods based on fuzzy techniques, neural networks the optimum gradient method have been proposed which given a good accuracy [38]. A P&O method to extract a maximum power based on fuzzy logic technique is reported in Ref. [45]. In Ref. [46], fuzzy logic controller as used to measure the power and rotational speed and then perturbs the operating speed by an optimal increment/decrement of rotor speed, with regard on power turbine variation in positive or negative direction. The P&O method is suitable for wind turbines with small inertia, but not for medium and large inertia wind turbine systems, since the P&O method adds a delay to the system control [43], and some of them are still complex to implement [38].

The third method named PSF (power signal feedback), is based on the wind turbine maximum power curve (maximum power versus shaft speed) allowing the maximum power tracking by shaft speed control [47]. Wind speed measurement is not required with this method [47–50]. However, experimentally measurement of the power versus turbine speed curves, performed off-line is usually required. The last method called OTC (optimum torque control) consists of the adjusting of the generator torque to the optimum value to different wind speed [30,51–53]. This MPPT strategy needs a look-up table of optimum torque or as a function on speed rotor. Also, with this method, the estimation of the generator can be required [53]. This method is not appropriate in medium or large wind turbine, since its inertia makes its response slow during a sudden and rapid changes in wind speed [30].

In this paper, in order to overcome the drawbacks of the conventional MPPT algorithms, a novel sensorless FLC MPPT (fuzzy logic maximum power point tracking) is presented. The proposed sensorless MPPT strategy has been applied to a wind turbine driving a DFIG operating at variable speed in which stator is directly connected to the distribution grid while the rotor windings are connected via a Pulse Width Modulation (PWM) back-to-back converter (see Fig. 1). The paper is organized as follows. Section 2 presents the dynamics models of both DFIG and wind turbine system. Focus is given only on the RSC (rotor side converter). Section 3 presents the control of the DFIG. Section 4 detailed the proposed sensorless MPPT strategy based on fuzzy logic techniques. The proposed control scheme is investigated according to wind speed variations and simulation results are presented in Section 5. The experimental test of controlling DC motor as the wind turbine emulator is presented in Section 6. Finally, conclusions about the effectiveness and the performance of the proposed sensorless FLC MPPT algorithm are outlined.

2. DFIG wind turbine model

2.1. DFIG model

Application of Concordia and Park's transformations to the three-phase model of the DFIG allows to write the dynamic voltages and fluxes equations in an arbitrary d-q reference frame [54–56]:

$$\begin{cases} v_{ds} = r_s i_{ds} + \dfrac{d\lambda_{ds}}{dt} - \omega_s \lambda_{qs} \\ v_{qs} = r_s i_{qs} + \dfrac{d\lambda_{qs}}{dt} + \omega_s \lambda_{ds} \\ v_{dr} = r_r i_{dr} + \dfrac{d\lambda_{dr}}{dt} - \omega_r \lambda_{qr} \\ v_{qr} = r_r i_{qr} + \dfrac{d\lambda_{qr}}{dt} + \omega_r \lambda_{dr} \end{cases} \quad (1)$$

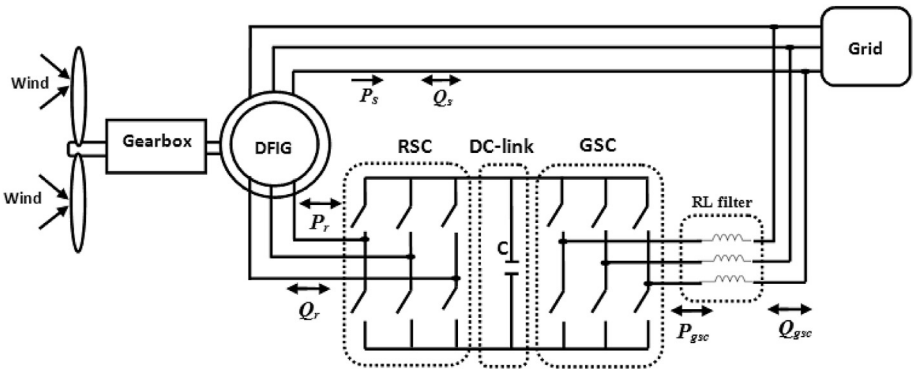

Fig. 1. General scheme of the wind energy conversion system.

where r_s and r_r are respectively the resistance of the stator and rotor windings, ω_s is the rotational speed of the synchronous reference frame, and ω_r the rotor reference frame rotating.

The flux linkages are given by:

$$\begin{cases} \lambda_{ds} = L_s i_{ds} + M i_{dr} \\ \lambda_{qs} = L_s i_{qs} + M i_{qr} \\ \lambda_{dr} = L_r i_{dr} + M i_{ds} \\ \lambda_{qr} = L_s i_{qs} + M i_{qr} \end{cases} \quad (2)$$

where L_s and L_r are respectively the inductances of the stator and rotor windings, and M is the mutual inductance.

By using Eqs. 1 and 2, the dynamic model of the DFIG can be expressed as:

$$\begin{cases} \dfrac{d\lambda_{ds}}{dt} = -\dfrac{r_s}{L_s} i_{ds} + \omega_s \lambda_{qs} + \dfrac{r_s}{L_s} M i_{dr} + V_{ds} \\ \dfrac{d\lambda_{ds}}{dt} = -\dfrac{r_s}{L_s} i_{qs} - \omega_s \lambda_{ds} + \dfrac{r_s}{L_s} M i_{qr} + V_{qs} \\ \dfrac{di_{dr}}{dt} = -\dfrac{r_r}{\sigma} i_{dr} + \omega_r \sigma i_{qr} - \dfrac{M}{L_s}\dfrac{d\lambda_{ds}}{dt} + \omega_r \dfrac{M}{L_s}\lambda_{qs} + V_{dr} \\ \dfrac{di_{qr}}{dt} = -\dfrac{r_r}{\sigma} i_{qr} - \omega_r \sigma i_{dr} - \dfrac{M}{L_s}\dfrac{d\lambda_{qs}}{dt} - \omega_r \dfrac{M}{L_s}\lambda_{ds} + V_{qr} \end{cases} \quad (3)$$

where $\sigma = L_r - M^2/L_s$ is the Blondel dispersion factor.

The electromagnetic torque of the DFIG can be expressed as follow:

$$T_{em} = P\frac{3}{2}\frac{M}{L_s}(\lambda_{ds} i_{qr} - \lambda_{qs} i_{dr}) \quad (4)$$

where P is the number of pole pairs.

By neglecting the power losses associated with the stator resistances, the active and reactive power can be expressed as [10]:

$$\begin{cases} P_s = \dfrac{3}{2}(v_{ds} i_{ds} + v_{qs} i_{qs}) \\ Q_s = \dfrac{3}{2}(v_{qs} i_{ds} - v_{ds} i_{qs}) \end{cases} \quad (5)$$

2.2. Wind turbine model

For a given wind speed v_w, the mechanical power P_m generated by the turbine is expressed as [17,18]:

$$P_m = \frac{1}{2}\rho A C_p(\lambda, \beta) v_w^3 \quad (6)$$

where ρ is the density of the air in kg/m^3; $A = \pi R^2$ is the area swept by blade in m2, and R the radius of the blade in m.

The aerodynamic model of a wind turbine can be determined by the $C_p(\lambda,\beta)$ curves. C_p is the power coefficient, which is a function of

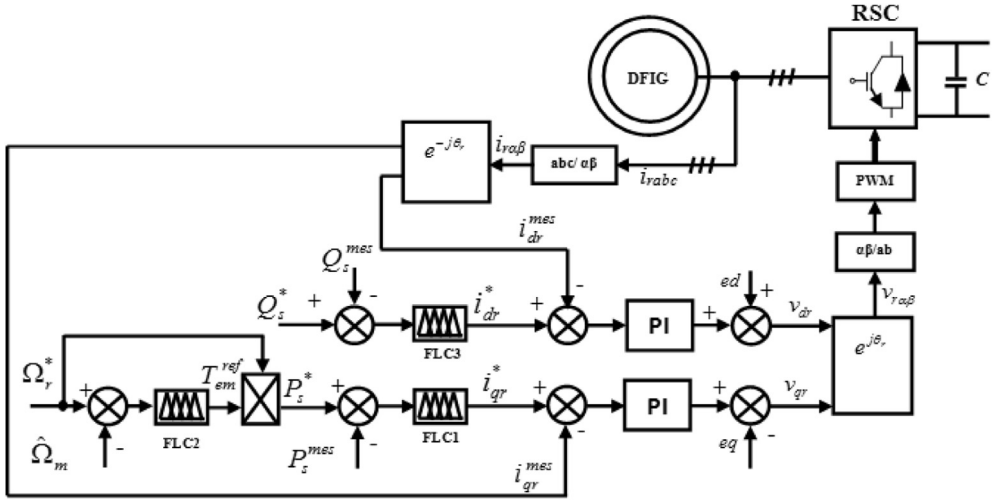

Fig. 2. Block diagram of the overall RSC control scheme.

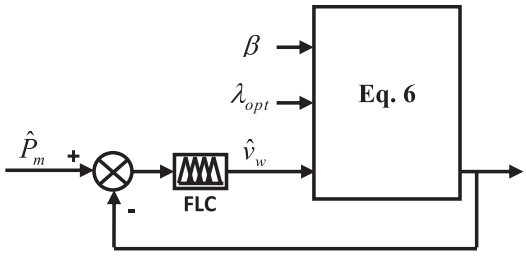

Fig. 3. Fuzzy technique based wind speed estimation (Revised).

both tip-speed-ratio λ and the blade pitch angle β. The tip-speed-ratio is given by:

$$\lambda = \frac{\Omega_r R}{v_w} \tag{7}$$

where Ω_r represents the rotational speed of the wind turbine in rad/sec.

Knowing the optimal tip-speed ratio (λ_{opt}), and the estimated wind speed$\widehat{v}_w$, the optimal DFIG speed to achieve a maximum wind power tracking is given by:

$$\Omega_r^* = \frac{\lambda_{opt}\widehat{v}_w}{R} \tag{8}$$

The power coefficient is non-dimensional term and is modeled by the following equation:

$$C_p = 0.398 \sin\left(\frac{\pi(\lambda - 3)}{15 - 0.3\beta}\right) - 0.00394(\lambda - 2)\beta \tag{9}$$

Generally, if the wind speed is below its rated value, the WTG operates in the variable speed mode, and C_p is kept at its maximum value. In this operating mode, the pitch control is deactivated. If the wind speed is above the rated value, the pitch control is activated in order to reduce the generated mechanical power [10].

3. DFIG control

In order to verify the effectiveness of the new proposed FLC MPPT algorithm, only the Rotor Side Converter Control is presented.

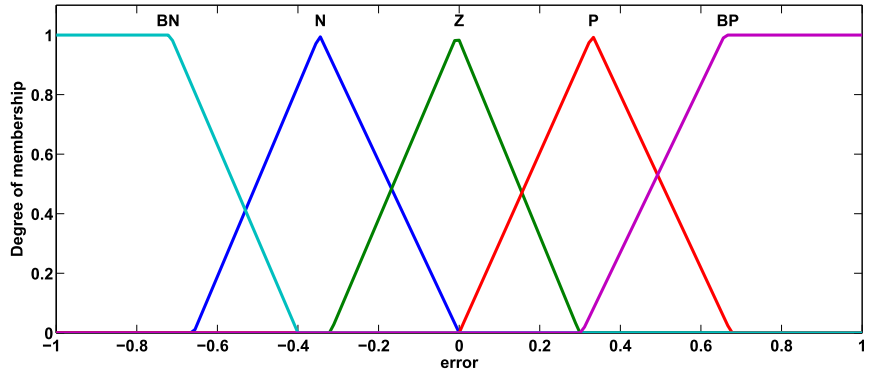

Fig. 4. Membership functions on inputs and output of the FLC wind speed estimator (Revised).

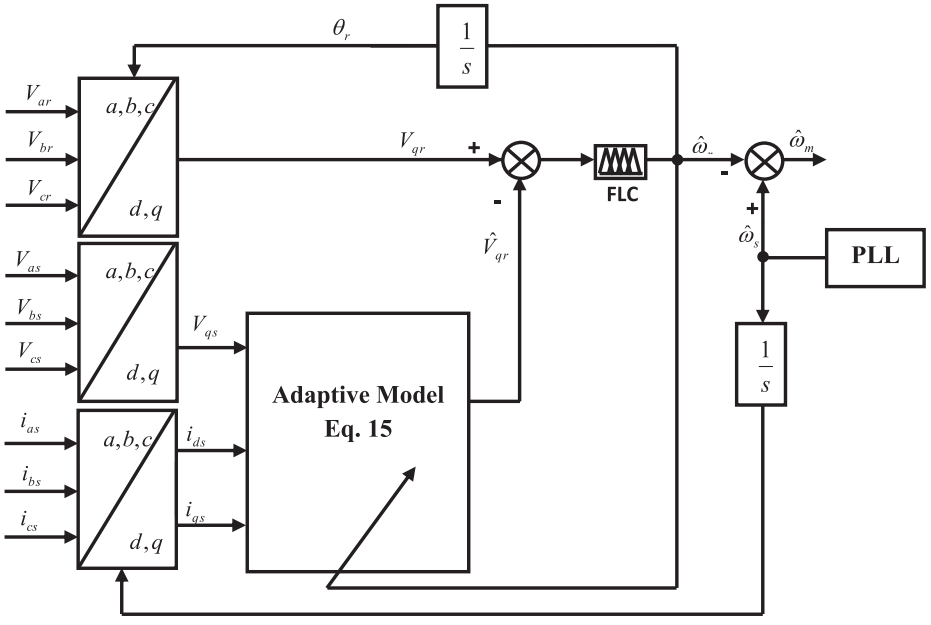

Fig. 5. Schematic blocks of the MRAS based DFIG rotor speed observer (Revised).

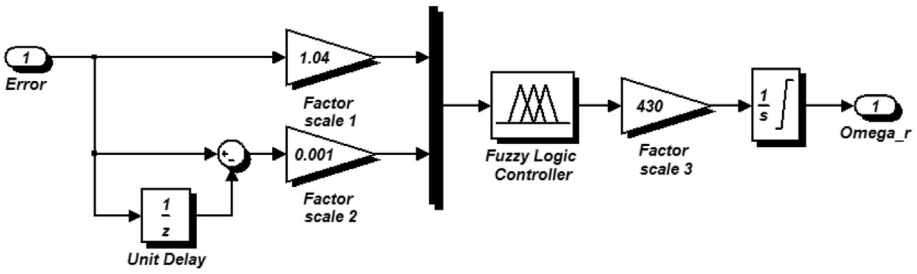

Fig. 6. Structure of fuzzy logic controller of MRAS observer.

Table 1
Wind speed estimator FLC rules base.

Output		Δe(t)				
		BN	N	Z	P	BP
e(t)	BN	BN	Z	BN	Z	Z
	N	Z	N	N	Z	Z
	Z	BN	N	Z	P	BP
	P	Z	Z	P	P	Z
	BP	Z	Z	BP	Z	BP

Table 2
MRAS FLC rules base.

Output		Δe(t)				
		BN	N	Z	P	BP
e(t)	BN	BN	Z	BN	Z	Z
	N	Z	N	N	Z	Z
	Z	BN	N	Z	P	BP
	P	Z	Z	P	P	Z
	BP	Z	Z	BP	Z	BP

The GSC (grid side converter) which is controlled to regulate the DC-link voltage and adjust the power factor, is largely investigated in the literature. The technique presented in Refs. [57–61] is used in this paper.

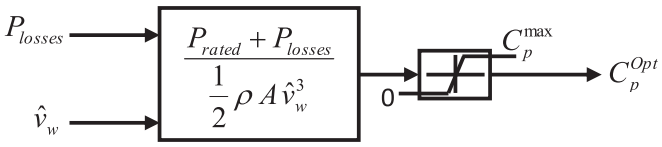

Fig. 8. Calculation of optimal power coefficient (Revised).

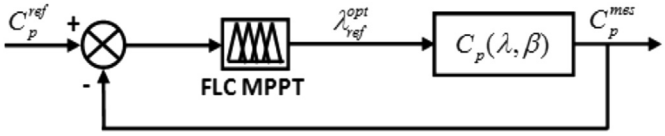

Fig. 9. Structure of the MPPT FLC.

Fig. 2 shows the overall vector control scheme of the RSC. Independent control of the generator rotor speed Ω_m^* and reactive power Q_s is achieved by the means of rotor current's regulation. The control of RSC consists of regulating the rotor speed and reactive power independently [18]. In this paper, there are two control loops; the inner loop controls the direct and quadratic axis rotor's current while the outer loop controls the rotor speed and stator reactive power which are used to generate the reference signals of the direct and quadratic axis current components. For the inner loop control, the gains of PI (proportional-integral) are determined by means poles placement method, while fuzzy logic controllers are used in the outer loop.

In order to achieve a power decoupling control, the vector control strategy was adopted, with stator field orientation. Reactive

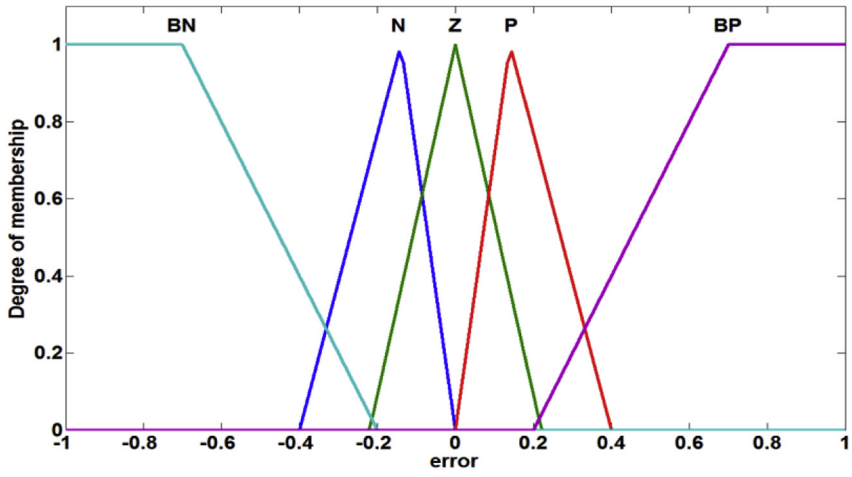

Fig. 7. Fuzzy membership functions for: voltage error, change of error of the rotor voltage, and the output of the DFIG rotor speed FLC estimation.

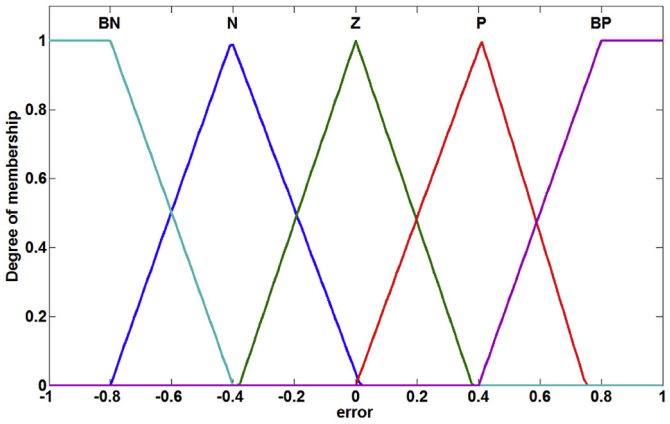

Fig. 10. Membership functions of error.

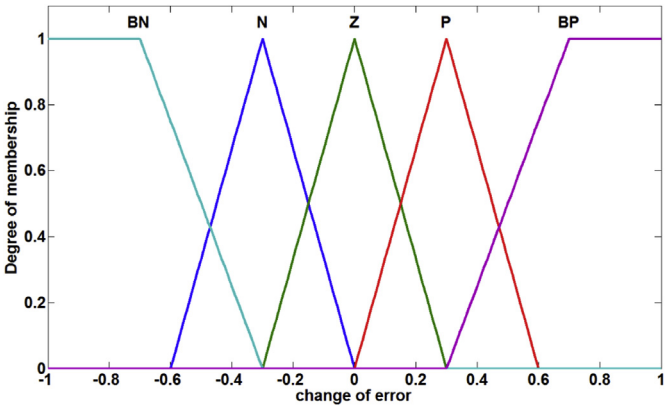

Fig. 13. Membership functions of the change of error.

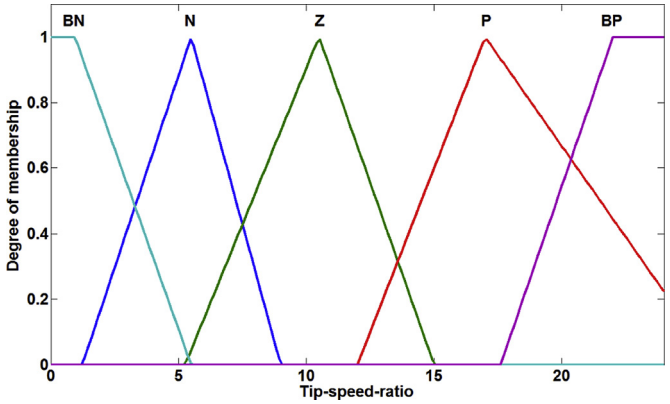

Fig. 11. Membership functions of the tip speed ratio.

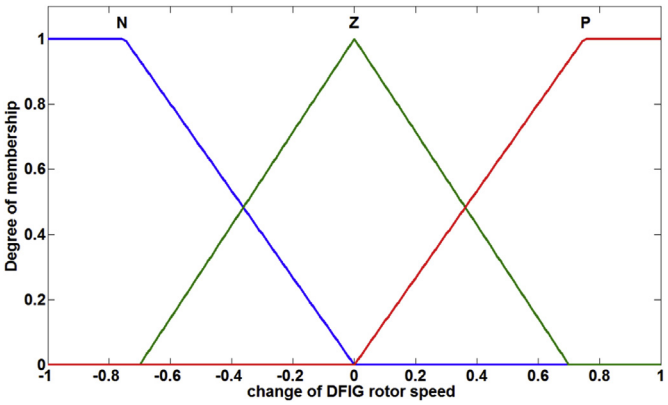

Fig. 14. Membership functions of the change of the DFIG rotor's speed.

power Q_s and generator speed are respectively proportional to rotor currents i_{dr} and i_{qr}.

4. Proposed FLC MPPT algorithm

4.1. Wind speed estimation

From the information about the wind turbine power, tip speed ratio and pitch blade angle β, the wind speed v_w can be calculated using roots or the nonlinear inverse function of Eq. (6). Generally, the lookup table method is used to implement an inverse function. Nevertheless, this method requires much memory space and may result in a time-consuming search for the solution. Moreover, the real-time calculation of nonlinear function roots may result in a complex and time consuming calculation, then reducing system performance [10]. The fuzzy technique, well known as a tool for nonlinear complex time-varying, can be an ideal technique to solve this problem [10].

In this paper, a wind speed estimation method based on the fuzzy technique is used. The method approximates the nonlinear inverse function of Eq. (6), as shown in Fig. 3. The membership

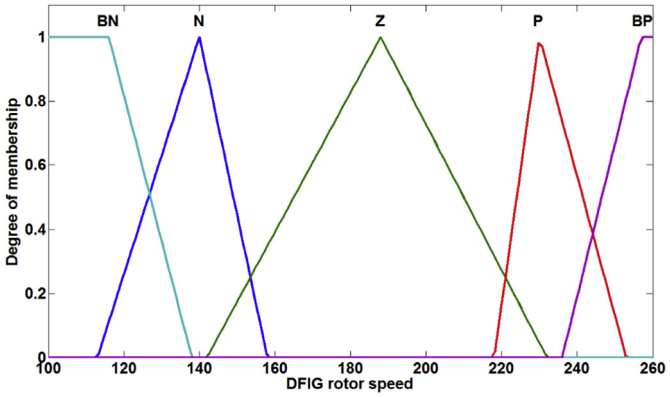

Fig. 12. Membership functions of the DFIG's speed.

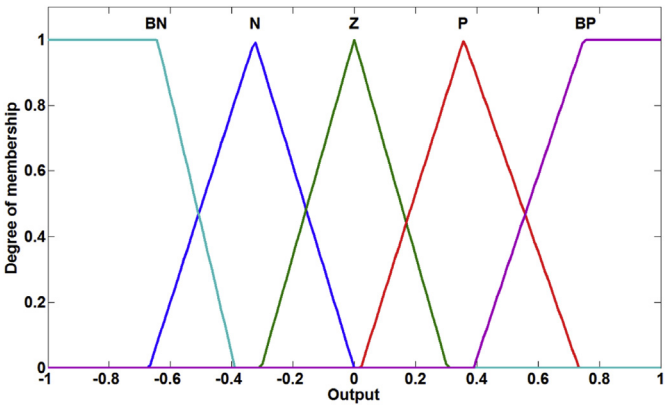

Fig. 15. Membership functions of the output.

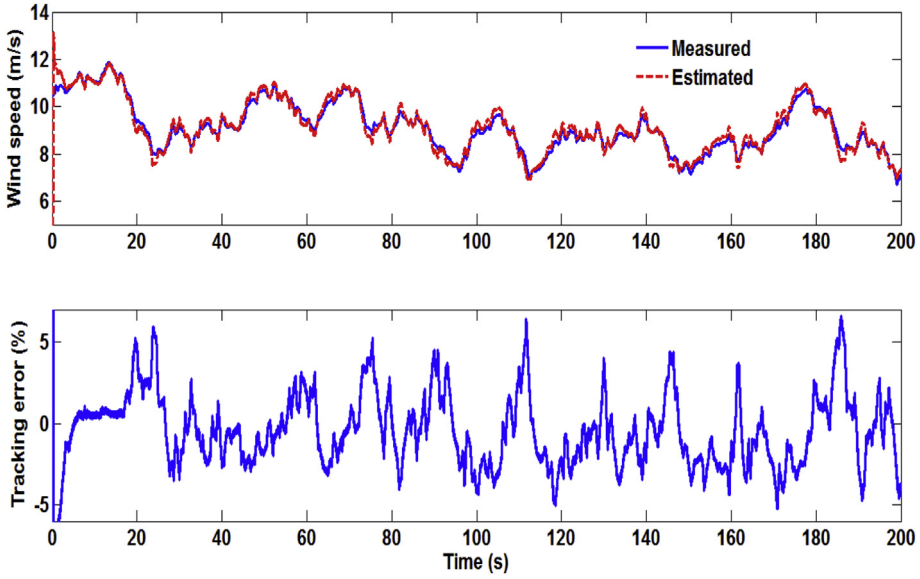

Fig. 16. Wind speed estimation.

functions of inputs and output of FLC (fuzzy logic maximum) used in Fig. 3 are shown in Fig. 4. Firstly, the turbine mechanical power is calculated from estimated DFIG's rotor speed given by MRAS observer which is presented in Section 4.2. The reference electromagnetic torque of the DFIG (T_{em}^{ref}) is given by the rotor speed controller (see Fig. 2), and by taking into account power losses in the gearbox [10]:

$$\Omega_m^* = G\Omega_r^* \tag{10}$$

where Ω_m^* represents the reference rotational speed of DFIG in rad/sec, G is the ratio of gearbox and Ω_r^* is the optimal speed of the turbine (Eq. (8)).

$$\widehat{P}_m = T_{em}^{ref}\widehat{\Omega}_m + P_{loss,GB} \tag{11}$$

$\widehat{P}_m$ is the estimated mechanical power, T_{em}^{ref} is the reference electromagnetic torque, $\widehat{\Omega}_m$ is the estimated DFIG rotor's speed, and $P_{loss,GB}$ is the power losses in the gearbox.

In order to provide an optimal DFIG rotor speed to achieve a maximum wind power tracking (Eq. (8)), the wind speed is estimated from the mechanical power. A fuzzy logic controller (which design is described in the previous section) gives the estimation of the wind speed, with the prerequisite knowledge of the tip speed ratio (λ_{opt}), blade pitch angle (β) (Eq. (6)).

4.2. DFIG rotor speed estimation

The proposed MRAS observer consists of using an adaptive model and a reference model in the closed loop scheme. A FLC is used in order to reduce the error between the two models.

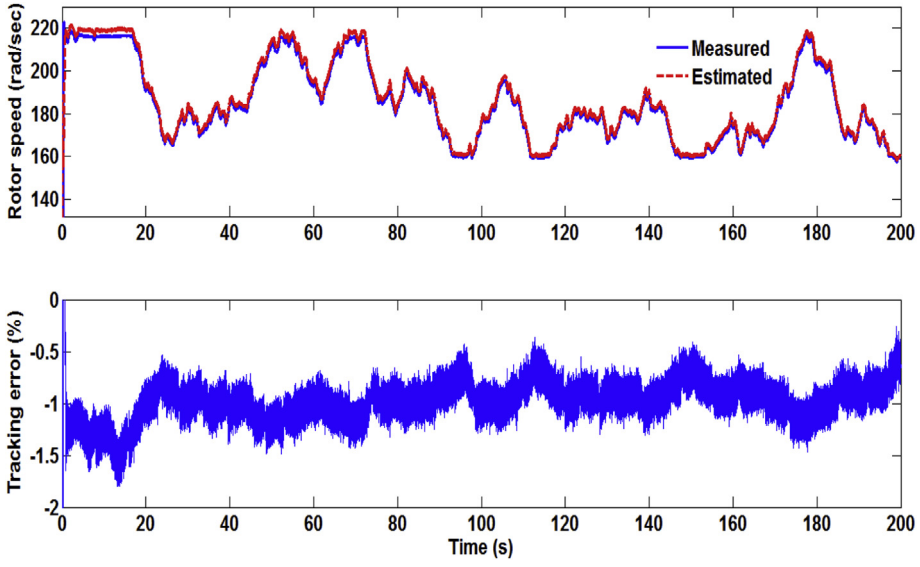

Fig. 17. DFIG rotor speed estimation performance using MRAS.

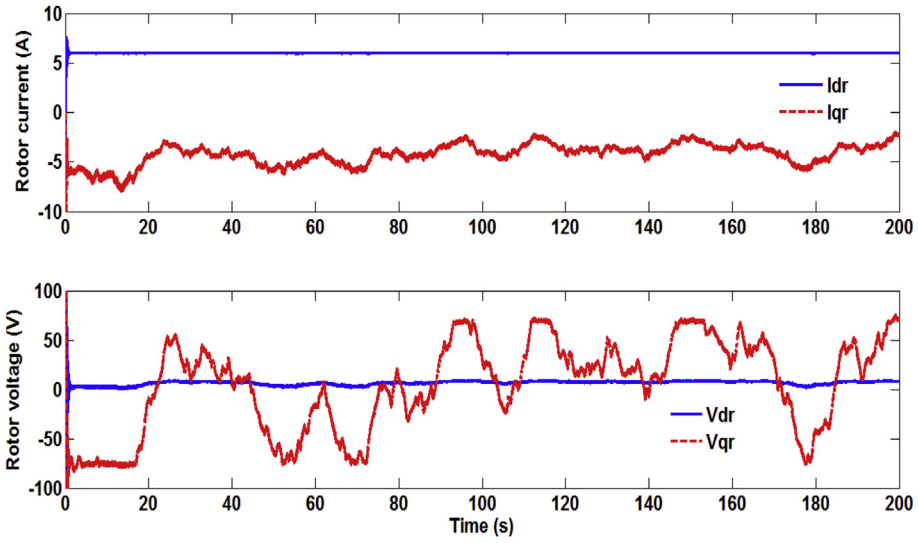

Fig. 18. DFIG rotor speed estimation.

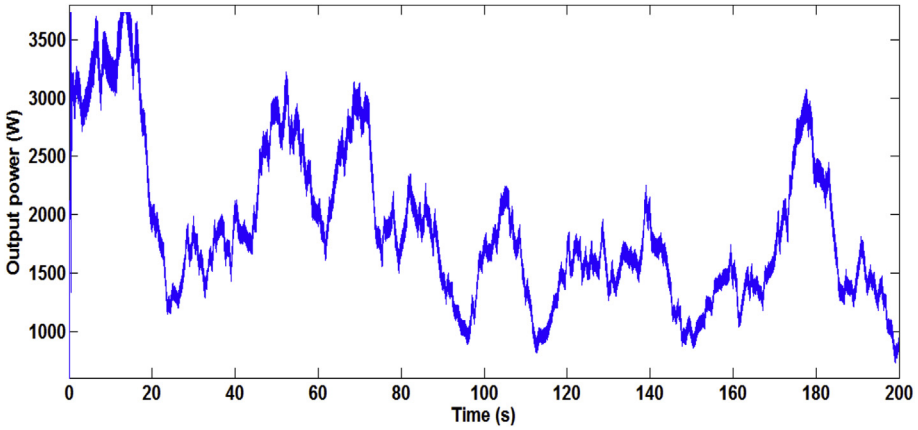

Fig. 19. Rotor current and voltage.

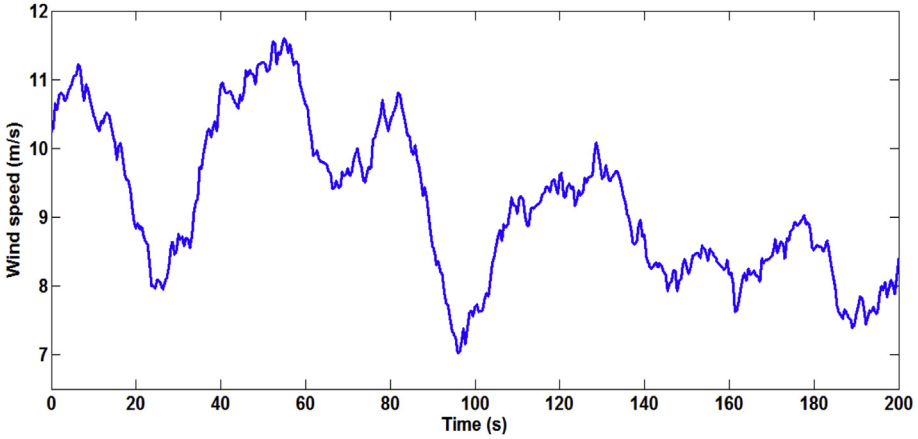

Fig. 20. Wind speed profile.

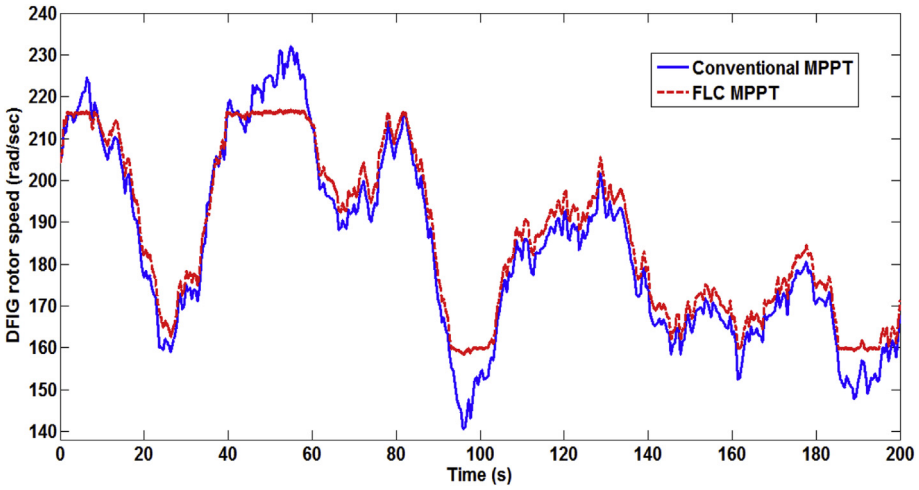

Fig. 21. Comparison of DFIG rotor speed for both MPPT strategies.

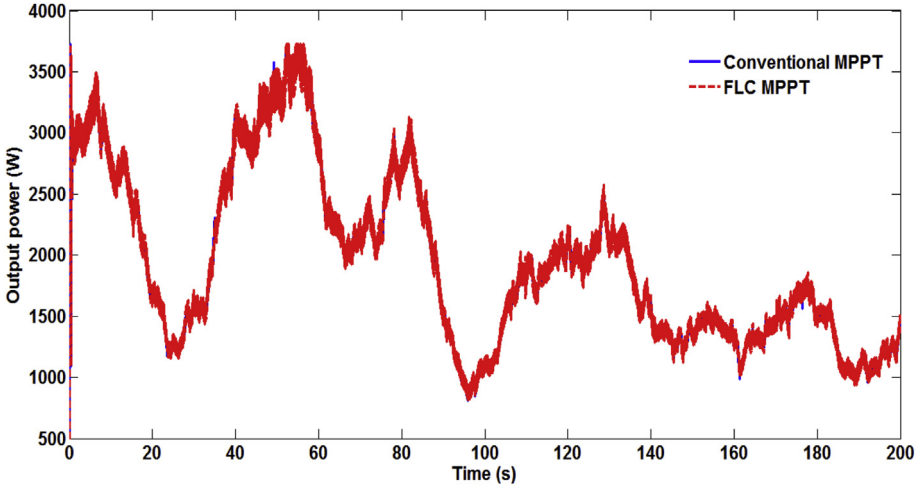

Fig. 22. Comparison of output power for both MPPT strategies.

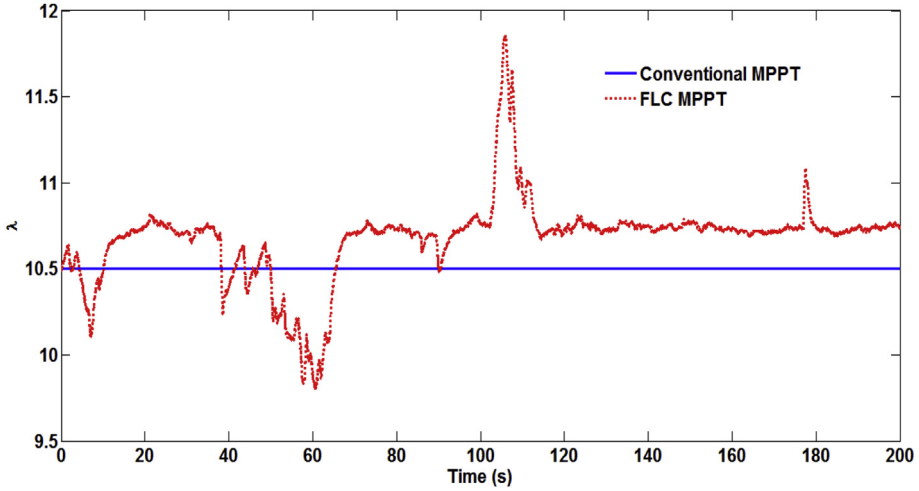

Fig. 23. Comparison of TSR for both MPPT strategies.

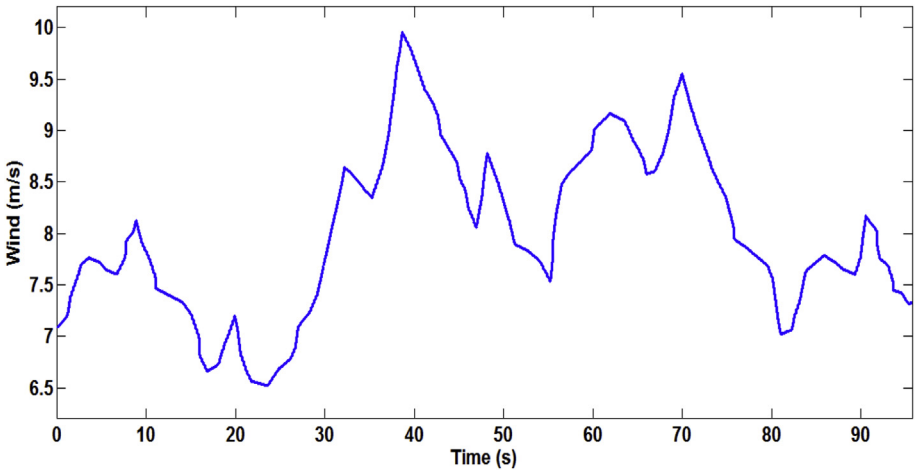

Fig. 24. Real wind speed profile.

Fig. 5 shows the overall scheme of the generator rotor position and speed estimation of the proposed method. From Eqs. (1) and (2), the q component of the rotor voltage and the d-axis rotor current can be expressed respectively as:

$$V_{qr} = r_r i_{qr} + L_r \frac{di_{qr}}{dt} + M \frac{di_{qs}}{dt} + \omega_r (L_r i_{dr} + M i_{ds}) \tag{12}$$

$$i_{dr} = \frac{1}{M}(\lambda_{ds} - L_s i_{ds}) \tag{13}$$

To achieve a power decoupling control, the vector control strategy is adopted, with a stator field orientation on the d-axis. As $\lambda_{qs} = 0$ in Eq. (2), the q component of the rotor current can be expressed as a function of the q component of the q-axis stator current as follow:

$$i_{qr} = -\frac{L_s}{M} i_{qs} \tag{14}$$

The estimated q-axis component of the rotor voltage used in the adaptive model can be written as:

$$\widehat{V}_{qr} = -\frac{r_r L_s}{M} i_{qs} + \left(M - \frac{L_r L_s}{M}\right) \frac{di_{qs}}{dt} + \widehat{\omega}_r \left(\left(\frac{L_r}{M}\lambda_{ds}\right) + \left(M - \frac{L_r L_s}{M}\right) i_{ds}\right) \tag{15}$$

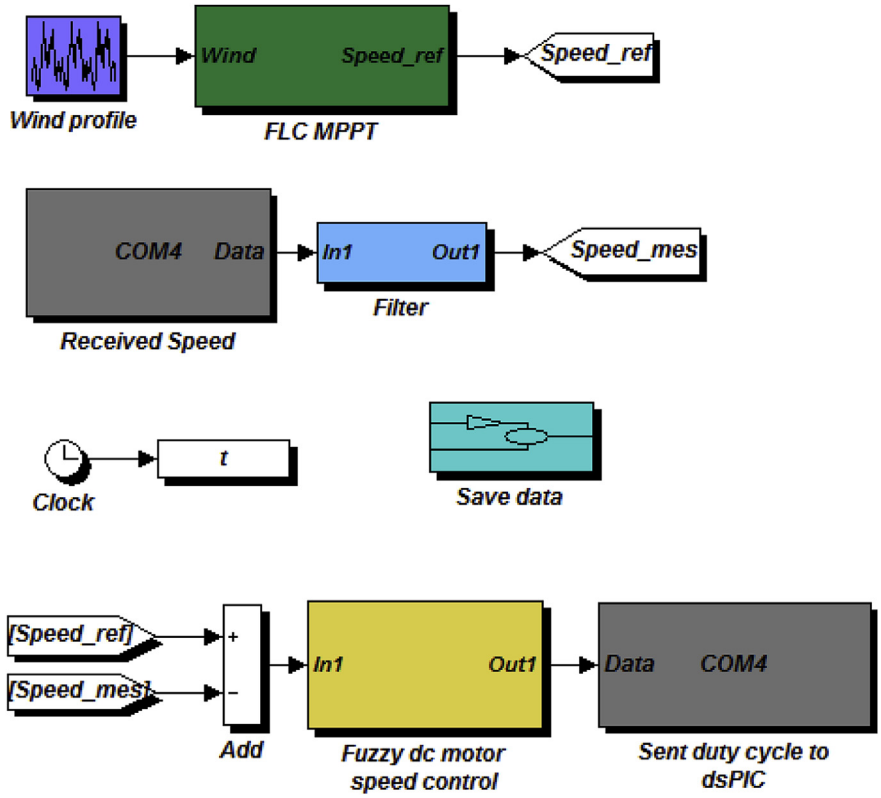

Fig. 25. Simulink scheme of MPPT control using serial communication.

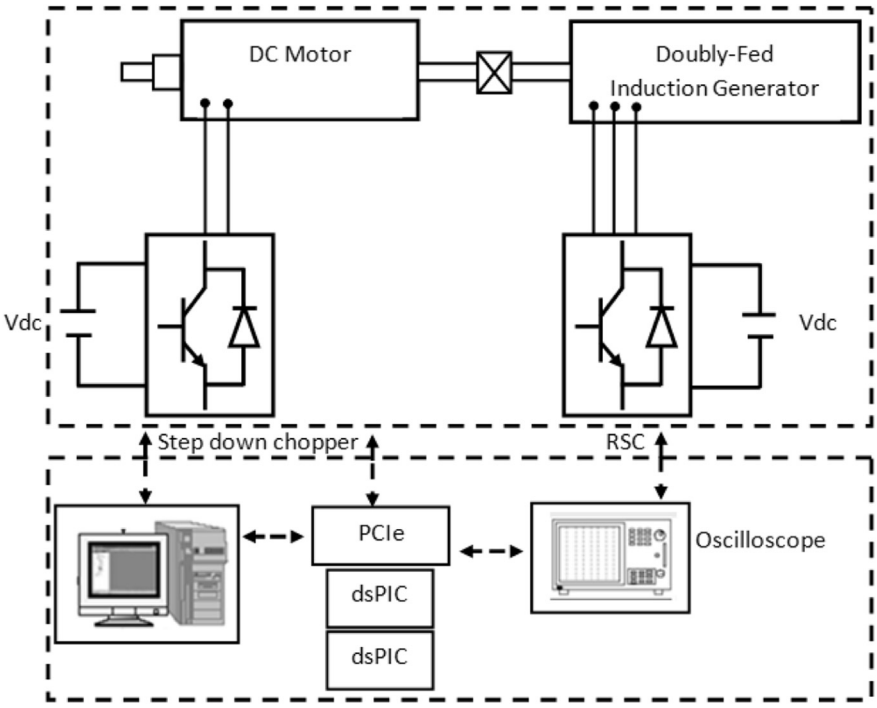

Fig. 26. Structure of the experimental test bench of wind emulator.

In order to estimate the rotational speed of the DFIG ($\widehat{\omega}_r$) using the MRAS observer, an increment/decrement fuzzy logic controller is used (as shown in Fig. 6). After estimating the rotor electrical angular velocity, the rotational speed of DFIG is estimated using the electrical frequency ω_s throughout PLL (phase-locked loop).

The fuzzy controller includes four parts [62]: fuzzification, fuzzy rule base, inference engine and defuzzification. There are two input signals to the FLC (fuzzy logic controller): the speed's error e and the change of the error Δe (Table 1). The error and change of error are converted by scaling factors (Fig. 6). To obtain the output of the FLC, the defuzzication used is based on the center of gravity method, and the triangular membership with overlap is used for the inputs and for the output of each FLC. The linguistic terms used for input–output membership functions are labeled as "*BN* (*Big Negative*)", "*N* (*Negative*)", "*Z* (*Zero*)", "*P* (*Positive*)", and "*BP* (*Big Positive*)". Table 2 illustrates the fuzzy inference rules of the rotor speed estimator. In order to improve the FLC's performance, an empirical analysis is used to set parameters of the membership. Fig. 7 depicts the membership functions for the input and output variables respectively.

4.3. Proposed sensorless MPPT algorithm

A sensorless MPPT solution based on fuzzy logic technique is proposed. The optimum value of power coefficient is provided by the estimation the overall power losses in the WTG and by using the estimated wind speed as showed in Fig. 8. The structure of the proposed FLC MPPT algorithm is shown in Fig. 9. The main advantage of this sensorless MPPT strategy is to track a maximum power point by reducing the size of PWM back-to-back converters by approximately 40% resulting in significant minimizing of converter losses and overall system's cost [63].

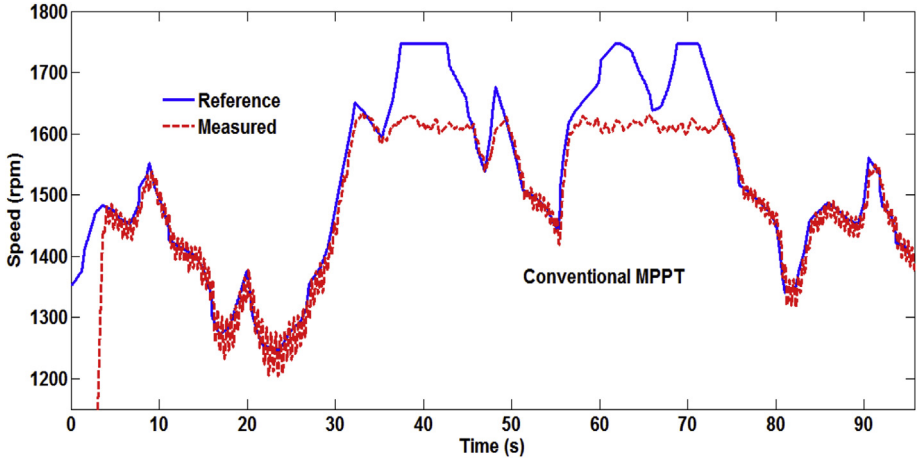

Fig. 27. Performance of the proposed wind emulator speed control algorithm.

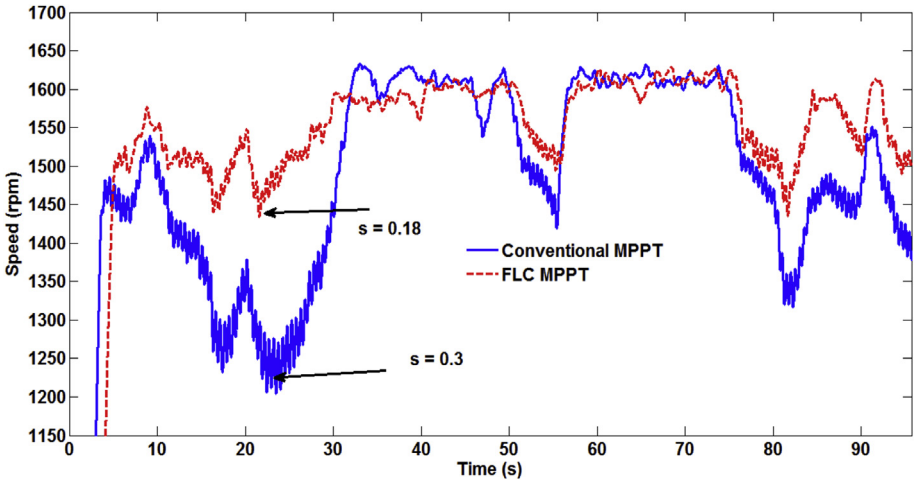

Fig. 28. Comparison of the measured speed of the wind emulator for both MPPT algorithms.

Firstly, for the adopted MPPT algorithm, the optimal value of the power coefficient by taking into account the power losses is expressed as (see Fig. 8):

$$C_p^{\text{opt}} = \frac{\widehat{P}_{\text{losses}} + P_{\text{rated}}}{2\rho A \widehat{v}_w^3} \tag{16}$$

where C_p^{opt} is the optimal power coefficient to extract the maximum wind power, $\widehat{v}_w$ is the estimated wind speed, $\widehat{P}_{\text{losses}}$ and P_{rated} are respectively the estimated power losses and the rated output power of DFIG. Note that the value of C_p^{opt} is kept at its maximum value when the provided power from the wind generator is under its rated power, while it is reduced if the output power is above its rated power.

Using the Eq. 16 and the value of blade pitch angle (which is determined by the Pitch Control system), the FLC MPPT algorithm calculates the value of the optimal tip speed ratio (λ_{opt}) which gives the optimal value of the power coefficient according to the estimated wind speed (see Fig. 8). The mathematical representation of the C_p curves used in this study is given in Eq. (8). Then, the optimal generator reference speed Ω_r^* for maximum wind power tracking is determined (Eq. (7)).

The structure of the fuzzy logic controller proposed for FLC MPPT is developed below. It contains five inputs: the error (Fig. 10), the previous value of the tip speed ratio λ (Fig. 11), the DFIG rotor's speed (Fig. 12), the change of error (Fig. 13), the change of the DFIG rotor's speed (Fig. 14) and the FLC output, which represents the optimal tip speed ratio λ_{opt} (Fig. 15).

Note that the FLC MPPT controller has been programmed in C code using an embedded S-function block in Matlab/Simulink software. Therefore, the hardware implementation of the proposed FLC MPPT algorithm can be achieved using a microcontroller or a DSP.

5. Results and discussion

In this paper, the performance and the effectiveness of a sensorless FLC MPPT technique have been evaluated on a WTG driving DFIG (Fig. 1) with parameters given in the Appendix. Simulation study has been carried out using Matlab/Simulink in order to emulate the wind variations, and to compare the performance of the proposed sensorless FLC MPPT algorithm with previously reported conventional method [27]. The Van der Hoven model of wind speed detailed in Ref. [64] is used in this study. Fig. 16 shows the measured and the estimated wind speed, where the tracking

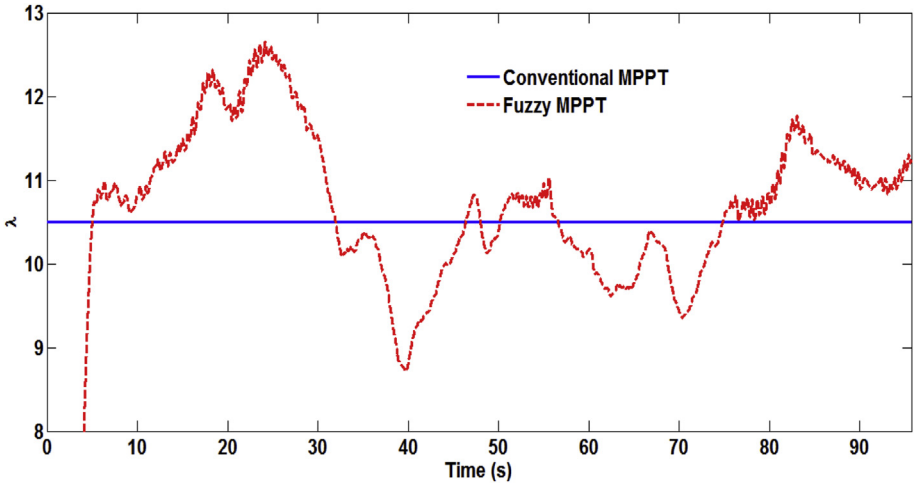

Fig. 29. Comparison of the variation of tip speed ratio for both MPPT algorithms.

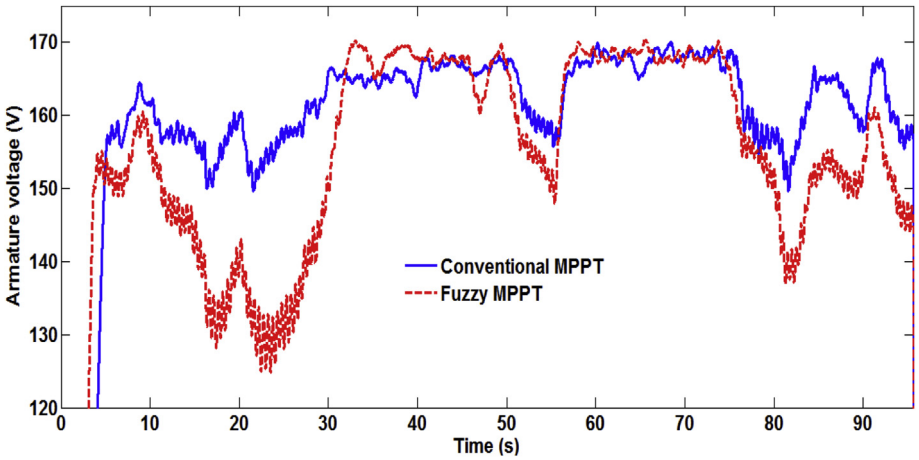

Fig. 30. Armature voltage for both MPPT algorithms.

error is less than ±6%. The performance of DFIG's rotor speed estimation by using MRAS observer is depicted in Fig. 17, where the tracking error is less than 2%. The direct and quadratic rotor current of DFIG is shown in Fig. 18. The output power is depicted in Fig. 19. In order to verify the effectiveness of the proposed sensorless FLC MPPT strategy, simulations have been carried out. Fig. 20 illustrates the wind speed profile where Fig. 21 depicts the comparison of DFIG rotor speed for both conventional and new FLC MPPT. The results indicate clearly a slower dynamic variation of the rotor speed in the FLC MPPT algorithm compared to the conventional one. With the new FLC MPPT strategy, the slip which is proportional to the size of power converters is reduced (about 40%). Then, the power converters can be downsized without reducing the output power provided as shown in Fig. 22. This leads to a decrease in both cost and maintenance of the overall system by reducing the size of the back-to-back converters. The comparison of the optimal tip speed ratio of both MPPT strategies is illustrated in Fig. 23.

6. Experimental validation

The experimental equipment which consists of the implementation of the control system for wind turbine composed of a DC motor, a microcontroller with the speed control algorithm and serial communication unit. The emulator has been tested in the laboratory to verify the effectiveness of our control strategy based on using Matlab/Simulink software and microcontroller through serial communication. A real wind speed illustrated in Fig. 24 is used to verify the performance of the DC motor control and new FLC MPPT. The Simulink scheme of the implementation of the new FLC MPPT algorithm using the Instrument Control Toolbox is shown in Fig. 25. Fig. 26 illustrates the global structure of the experimental test bench.

The emulator includes a 3.7 kW rated power dc motor whose parameters are given in Appendix. In order to control the speed of the emulator, a microcontroller (dsPIC 33FJ12MC202) is used to regulate the dc–dc chopper output voltage. Simulink model computes the duty cycle and sent it to microcontroller, and receives the measured speed data via RS232 serial communication protocol. The performance of the proposed fuzzy logic speed control using serial communication port is illustrated in Fig. 27, where the measured speed tracks well the reference speed, and the tracking error is less than 4%. The measured speed is limited to 1620 rpm due the limitation of the DC voltage source of step down chopper to 175 V. The rated voltage of DC motor is 240 V Fig. 28, shows the comparison of the measured speed of the wind emulator for both MPPT algorithms. As we can see, with the FLC MPPT, the slip of generator is reduced by 40% approximately, which means the same downsizing of the used back-to-back power converters. Fig. 29 illustrates the variation of TSR for both MPPT algorithms. In the case of FLC MPPT, the value of TSR changes (around 10.5 which is its optimal value) in order to track the maximum power point. The variations of TSR are due to the fast change of the wind speed and the relatively slow responses of the wind turbine system. The armature voltage for both MPPT algorithms is depicted in Fig. 30. The experimental results illustrate the effectiveness of the wind emulator speed control by using the Simulink interface and a microcontroller with serial communication. Indeed, in order to save the memory of microcontroller and make easy the implementation of the proposed algorithm, the control strategy proposed in this paper is suitable and feasible.

7. Conclusions

A study of a wind speed estimation based on sensorless maximum power extracting for a variable speed WTG system was conducted in this paper. The proposed control system has been investigated for a wind turbine driving a DFIG. To provide a maximum output power according to the variation of wind speed, a Fuzzy Logic MPPT algorithm is used. This new FLC MPPT method provides the same output electrical power compared to the conventional MPPT method, while the size of power converter is reduced by around 40%.

The mechanical power is estimated from the estimation of the DFIG rotor speed based on the MRAS observer and the electromagnetic reference torque given by the rotor speed controller. The wind speed is then estimated from the mechanical power using a fuzzy logic controller. Simulation results highlight that this approach has better performance compared to the conventional method that uses both output power and estimation the overall power losses.

Verification of the proposed sensorless control system has been carried out by performing some simulations on a 190 kW WTG system. The results have shown that both wind speed and DFIG rotor speed were estimated with a good accuracy. The resulting WTG system provided maximum electrical output power to the grid with a reduced size of the converters and system's cost without using mechanical anemometers.

In the aim to verify the effectiveness of the FLC MPPT proposed in this work, a feasible and easy method using Simulink interface and microcontroller which exchanging data through serial RS232 communication are presented and tested successfully. This method

permits to regulate the speed of DC motor and accomplish the MPPT strategy using fuzzy logic techniques.

Acknowledgments

This work has been supported by the Hydro-Québec LTE, H2CAN Network, Natural Resources Canada and the Natural Sciences and Engineering Research Council of Canada.

Appendix

Wind turbine rated capacity = 3.7 kW, number of blades = 3, rotor diameter = 2.1 m, swept area = 13.85 m^2, cut-in wind speed = 4 m/s, cut-out wind speed = 25 m/s.

Wound rotor induction generator: rated power = 3.7 kW, stator rated voltage = 380 V, number of pair of poles = 2, R_s = 1.115 Ω, R_r = 1.083Ω, M = 0.2037 mH, L_s = 0.02096 mH, L_r = 0.02096 mH, base frequency = 60 Hz, dc-link capacitor: 3.5 mF.

DC motor rated power = 3.7 kW, R_a = 1.7 Ω, L_a = 29.8 mH, J = 0.00541 kg/m^2, f = 0.006 N.m.s.

References

[1] Banos R, Manzano-Agugliaro F, Montoya F, Gil C, Alcayde A, Gómez J. Optimization methods applied to renewable and sustainable energy: a review. Renew Sustain Energy Rev 2011;15(4):1753–66.
[2] Hong-Hee L, Phan Quoc D, Le Minh P, Le Dinh K, Nguyen Huu N. A new fuzzy logic approach for control system of wind turbine with doubly fed induction generator. Conference A new fuzzy logic approach for control system of wind turbine with doubly fed induction Generator. p. 134–139.
[3] Xingjia Y, Chuanbao Y, Deng y, Jiasi G, Lina Y. The grid-side PWM converter of the wind power generation system based on fuzzy sliding mode control. Conference the grid-side PWM converter of the wind power generation system based on fuzzy sliding mode control. p. 973–978.
[4] González LG, Figueres E, Garcerá G, Carranza O. Maximum-power-point tracking with reduced mechanical stress applied to wind-energy-conversion-systems. Appl Energy 2010;87(7):2304–12.
[5] Hernández-Escobedo Q, Saldaña-Flores R, Rodríguez-García E, Manzano-Agugliaro F. Wind energy resource in Northern Mexico. Renew Sustain Energy Rev 2014;32:890–914.
[6] Montoya FG, Aguilera MJ, Manzano-Agugliaro F. Renewable energy production in Spain: a review. Renew Sustain Energy Rev 2014;33(0):509–31.
[7] Association WWE. World wind energy report 2008. Bonn: WWEA; 2009.
[8] Zhiqiang X, Qinghua H, Ehsani M. Estimation of effective wind speed for fixed-speed wind turbines based on frequency domain data fusion. Sustain Energy IEEE Trans 2012;3(1):57–64.
[9] Tan K, Islam S. Optimum control strategies in energy conversion of PMSG wind turbine system without mechanical sensors. Energy Convers IEEE Trans 2004;19(2):392–9.
[10] Wei Q, Wei Z, Aller JM, Harley RG. Wind speed estimation based sensorless output maximization control for a wind turbine driving a DFIG. Power Electron IEEE Trans 2008;23(3):1156–69.
[11] Meyer DG, Srinivasan S, Semrau G. Dynamic wind estimation based control for small wind turbines. Renew Energy 2013;50:259–67.
[12] Kodama N, Matsuzaka T, Tuchiya K, Arinaga S. Power variation control of a wind generator by using feed forward control. Renew energy 1999;16(1):847–50.
[13] Van der Hooft E, Van Engelen T. Estimated wind speed feed forward control for wind turbine operation optimisation. Conference estimated wind speed feed forward control for wind turbine operation optimisation.
[14] Boukhezzar B, Siguerdidjane H. Nonlinear control with wind estimation of a DFIG variable speed wind turbine for power capture optimization. Energy Convers Manag 2009;50(4):885–92.
[15] Mohandes M, Rehman S, Rahman SM. Estimation of wind speed profile using adaptive neuro-fuzzy inference system (ANFIS). Appl Energy 2011;88(11):4024–32.
[16] Vas P. Sensorless vector and direct torque control. Oxford, UK: Oxford university press; 1998.
[17] Munteanu I, Bratcu AI, Cutululis N-A, Ceanga E. Optimal control of wind energy systems: towards a global approach. Springer; 2008.
[18] Miller NW, Sanchez-Gasca JJ, Price WW, Delmerico RW. Dynamic modeling of GE 1.5 and 3.6 MW wind turbine-generators for stability simulations. Conference Dynamic modeling of GE 1.5 and 3.6 MW wind turbine-generators for stability simulations, vol. 3. p. 1977–1983.
[19] Phakamach P. Design of a fuzzy logic sliding mode model following controller for a Brushless DC Servomotor drivers. Energy Research Journal. 2(1):22–28.
[20] Hinkkanen M. Analysis and design of full-order flux observers for sensorless induction motors. Industrial Electron IEEE Trans 2004;51(5):1033–40.
[21] Lin W-M, Hong C-M, Cheng F-S. On-line designed hybrid controller with adaptive observer for variable-speed wind generation system. Energy 2010;35(7):3022–30.
[22] Song Z, Shi T, Xia C, Chen W. A novel adaptive control scheme for dynamic performance improvement of DFIG-based wind turbines. Energy 2012;38(1):104–17.
[23] Forchetti DG, Garcia GO, Valla MI. Adaptive observer for sensorless control of stand-alone doubly fed induction generator. Indus Electron IEEE Trans 2009;56(10):4174–80.
[24] Brahmi J, Krichen L, Ouali A. A comparative study between three sensorless control strategies for PMSG in wind energy conversion system. Appl Energy 2009;86(9):1565–73.
[25] Cardenas R, Pena R, Proboste J, Asher G, Clare J. MRAS observer for sensorless control of standalone doubly fed induction generators. Energy Convers IEEE Trans 2005;20(4):710–8.
[26] Dadone A, Dambrosio L. Estimator based adaptive fuzzy logic control technique for a wind turbine–generator system. Energy Convers Manag 2003;44(1):135–53.
[27] Lin W-M, Hong C-M, Cheng F-S. Design of intelligent controllers for wind generation system with sensorless maximum wind energy control. Energy Convers Manag 2011;52(2):1086–96.
[28] Montoya FG, Manzano-Agugliaro F, López-Márquez S, Hernández-Escobedo Q, Gil C. Wind turbine selection for wind farm layout using multi-objective evolutionary algorithms. Expert Syst Appl 1 November 2014;41(15):6585–95.
[29] Thongam JS, Ouhrouche M. MPPT control methods in wind energy conversion systems. Fundam Adv Top Wind Power 2011:339–60.
[30] Thongam J, Tarbouchi M, Beguenane R, Okou A, Merabet A, Bouchard P. An optimum speed MPPT controller for variable speed PMSG wind energy conversion systems. Conference an optimum speed MPPT controller for variable speed PMSG wind energy conversion systems. IEEE, p. 4293–4297.
[31] Barakati SM, Kazerani M, Aplevich JD. Maximum power tracking control for a wind turbine system including a matrix converter. Energy Convers IEEE Trans 2009;24(3):705–13.
[32] Abdullah M, Yatim A, Tan C, Saidur R. A review of maximum power point tracking algorithms for wind energy systems. Renew Sustain Energy Rev 2012;16(5):3220–7.
[33] Abo-Khalil AG, Dong-Choon L. MPPT control of wind generation systems based on estimated wind speed using SVR. Indus Electron IEEE Trans 2008;55(3):1489–90.
[34] Bhowmik S, Spee R, Enslin JHR. Performance optimization for doubly-fed wind power generation systems. Conference Performance optimization for doubly-fed wind power generation systems, vol. 3. p. 2387–2394.
[35] Hui L, Shi KL, McLaren PG. Neural-network-based sensorless maximum wind energy capture with compensated power coefficient. Indus Appl IEEE Trans 2005;41(6):1548–56.
[36] Cirrincione M, Pucci M, Vitale G. Growing neural Gas (GNG)-Based maximum power Point tracking for high-performance wind generator with an induction machine. Indus Appl IEEE Trans 2011;47(2):861–72.
[37] Hong C-M, Ou T-C, Lu K-H. Development of intelligent MPPT (maximum power point tracking) control for a grid-connected hybrid power generation system. Energy 2013;50:270–9.
[38] Ou T-C, Hong C-M. Dynamic operation and control of microgrid hybrid power systems. Energy 2014;66:314–23.
[39] Liyan Q, Wei Q. Constant power control of DFIG wind turbines with supercapacitor Energy storage. Indus Appl IEEE Trans 2011;47(1):359–67.
[40] Reza Kalantarian S, Heydari H. An analytical method for selecting optimized crowbar for DFIG with AHP algorithm. Conference an analytical method for selecting optimized crowbar for DFIG with AHP algorithm. p. 1–4.
[41] Simoes MG, Bose BK, Spiegel RJ. Design and performance evaluation of a fuzzy-logic-based variable-speed wind generation system. Indus Appl IEEE Trans 1997;33(4):956–65.
[42] Datta R, Ranganathan VT. A method of tracking the peak power points for a variable speed wind energy conversion system. Energy Convers IEEE Trans 2003;18(1):163–8.
[43] Quincy W, Liuchen C. An intelligent maximum power extraction algorithm for inverter-based variable speed wind turbine systems. Power Electron IEEE Trans 2004;19(5):1242–9.
[44] Tinglong P, Zhicheng J, Zhenhua J. Maximum power point tracking of wind Energy conversion systems based on sliding mode extremum seeking control. Conference maximum power Point tracking of wind Energy conversion systems based on sliding mode Extremum Seeking Control. p. 1–5.
[45] Bezza M, Moussaoui B, Fakkar A. Sensorless MPPT fuzzy controller for DFIG wind turbine. Energy Procedia 2012;18:339–48.
[46] Abdeddaim S, Betka A. Optimal tracking and robust power control of the DFIG wind turbine. Int J Electr Power Energy Syst 2013;49:234–42.
[47] Geng H, Yang G. A novel control strategy of MPPT taking dynamics of wind turbine into account. Conference a novel control strategy of MPPT taking dynamics of wind Turbine into Account. p. 1–6.
[48] Pena R, Clare JC, Asher GM. Doubly fed induction generator using back-to-back PWM converters and its application to variable-speed wind-energy generation. Electr Power Appl IEE Proc 1996;143(3):231–41.
[49] Valtchev V, Van den Bossche A, Ghijselen J, Melkebeek J. Autonomous renewable energy conversion system. Renew energy 2000;19(1):259–75.

[50] Muljadi E, Butterfield CP. Pitch-controlled variable-speed wind turbine generation. Industry Appl IEEE Trans 2001;37(1):240–6.
[51] Morimoto S, Nakayama H, Sanada M, Takeda Y. Sensorless output maximization control for variable-speed wind generation system using IPMSG. Conference Sensorless output maximization control for variable-speed wind generation system using IPMSG, vol. 3. p. 1464–1471.
[52] Ching-Tsai P, Yu-Ling J. A novel sensorless MPPT controller for a high-efficiency microscale wind power generation system. Energy Convers IEEE Trans 2010;25(1):207–16.
[53] Cardenas R, Pena R. Sensorless vector control of induction machines for variable-speed wind energy applications. Energy Convers IEEE Trans 2004;19(1):196–205.
[54] Ghennam T, Berkouk EM, Francois B. Modeling and control of a doubly fed induction generator (DFIG) based wind conversion system. Conference modeling and control of a Doubly Fed Induction Generator (DFIG) based Wind Conversion System. p. 507–512.
[55] Song Z, Xia C, Shi T. Assessing transient response of DFIG based wind turbines during voltage dips regarding main flux saturation and rotor deep-bar effect. Appl Energy 2010;87(10):3283–93.
[56] Morren J, De Haan SWH. Ridethrough of wind turbines with doubly-fed induction generator during a voltage dip. Energy Convers IEEE Trans 2005;20(2):435–41.
[57] Hu J, He Y, Xu L, Williams BW. Improved control of DFIG systems during network unbalance using PI–R current regulators. Industrial Electron IEEE Trans 2009;56(2):439–51.
[58] Fan L, Kavasseri R, Miao ZL, Zhu C. Modeling of DFIG-based wind farms for SSR analysis. Power Deliv IEEE Trans 2010;25(4):2073–82.
[59] Zhou P, He Y, Sun D. Improved direct power control of a DFIG-based wind turbine during network unbalance. Power Electron IEEE Trans 2009;24(11):2465–74.
[60] Mohseni M, Islam S, Masoum MA. Impacts of symmetrical and asymmetrical voltage sags on DFIG-based wind turbines considering phase-angle jump, voltage recovery, and sag parameters. Power Electron IEEE Trans 2011;26(5):1587–98.
[61] Hachicha F, Krichen L. Rotor power control in doubly fed induction generator wind turbine under grid faults. Energy 2012;44(1):853–61.
[62] Kalantar M, Mousavi GS. Dynamic behavior of a stand-alone hybrid power generation system of wind turbine, microturbine, solar array and battery storage. Appl Energy 2010;87(10):3051–64.
[63] Petersson A. Analysis, modeling and control of doubly-fed induction generators for wind turbines. Chalmers University of Technology; 2005.
[64] Nichita C, Luca D, Dakyo B, Ceanga E. Large band simulation of the wind speed for real time wind turbine simulators. Energy Convers IEEE Trans 2002;17(4):523–9.